Polymer Testing 103 (2021) 107364

Contents lists available at ScienceDirect

Polymer Testing

journal homepage: www.elsevier.com/locate/polytest

Influence of chemistry and fiber diameter of electrospun PLA, PCL and their blend membranes, intended as cell supports, on their biological behavior

María Herrero-Herrero [a,1], Sara Alberdi-Torres [b,1], Maria Luisa González-Fernández [b,1], Guillermo Vilariño-Feltrer [a], José Carlos Rodríguez-Hernández [a], Ana Vallés-Lluch [a,c], Vega Villar-Suárez [b,*]

[a] Centre for Biomaterials and Tissue Engineering, Universitat Politècnica de València, Cno. de Vera s/n, 46022, Valencia, Spain
[b] Institute of Biomedicine IBIOMED, Department of Anatomy, University of León-Universidad de León, Campus de Vegazana s/n, 24071, León, Spain
[c] Biomedical Research Networking Centre in Bioengineering, Biomaterials and Nanomedicine CIBER-BBN, Valencia, Spain

ARTICLE INFO

Keywords:
Tissue engineering
Adipose tissue derived-mesenchymal stem cells
PLA
PCL
Electrospinning
Chondrogenic differentiation

ABSTRACT

The prevalence of osteoarthritis, a degenerative cartilage disease that causes joint surface erosion and loss of mobility, emphasizes the need of producing a functional articular cartilage replacement. Tissue engineering has been the focus of recent research as a possible strategy for cartilage regeneration and repair. The most widely used technique for the manufacture of nanofibers is polymer electrospinning. Polylactic acid (PLA) and polycaprolactone (PCL) have been proved particularly suitable for nanofiber preparation, with many biomedical applications. The main aim of this work was to evaluate the behavior of adipose tissue-derived mesenchymal stem cells (ASCs) cultured on biomaterials of PLA, PCL and a combination of both (PLA/PCL), manufactured by electrospinning. We analyzed the bioactive properties of these cells in cultures on them, in terms of proliferation, adhesion, morphology, viability and differentiation. In addition, the influence of the thickness of the fibers in each biomaterial on these cellular characteristics was evaluated for their use in Cartilage Regenerative Medicine applications to promote chondrogenic differentiation. Depending on the parameter assessed, different results were obtained on each biomaterial. Using both polymers successful results on cellular viability were obtained, although in the case of PCL the cellular response in all the experiments was significantly better. As for the blends, positive outcomes were obtained, but they did not overtake the characteristics of PCL. Interestingly, ASCs were able to differentiate into chondrocytes without adding specific chondrogenic media in the three biomaterials tested. Moreover, a marked cell differentiation on PCL with 1.8 μm-fiber diameter and PLA/PCL blends was observed. These findings may play a key role in cartilage Regenerative Medicine and Tissue Engineering.

1. Introduction

Regenerative Medicine is a multidisciplinary science that encompasses principles of engineering and life sciences in order to achieve the functional regeneration of diseased or injured tissues and organs [1]. Tissue Engineering is a part of Regenerative Medicine science that combines supporting materials or structures (scaffolds), with biologically active cells and molecules in functional tissues for the same purpose, *i.e.* to restore, maintain or enhance damaged tissues or organs [2]. In Tissue Engineering strategies two fundamental components have to be developed and combined: the materials used as scaffolds and the cells that will colonise these materials [3].

Tissue Engineering makes use of many different cell types from which, at first, the most common were adult cells from different tissues (autologous or heterologous) grown on different biomaterials in order to obtain a biological substitute that could solve some kind of defect or disease [4]. However, these cells have a number of disadvantages, such as their low capacity for proliferation and differentiation, which promote the use of mesenchymal stem cells (MSCs), which make up for the deficiencies of adult cells. The main source of this type of cells is bone marrow (BMSCs), although these cells are also found in many tissues, such as adipose tissue. Mesenchymal stem cells derived from adipose tissue (ASCs) are considered a very promising alternative due to their easy obtaining, availability and their capacity of expansion and

* Corresponding author.
E-mail address: vega.villar@unileon.es (V. Villar-Suárez).
[1] María Herrero-Herrero, Sara Alberdi-Torres and Maria Luisa González-Fernández contributed equally to this work.

https://doi.org/10.1016/j.polymertesting.2021.107364
Received 26 May 2021; Received in revised form 14 September 2021; Accepted 24 September 2021
Available online 30 September 2021

proliferation [5]. In addition, ASCs have low immunogenicity and are able to evade the immune response [6]. As a consequence of the various advances in molecular biology over the years, much knowledge has been acquired about the genetic mechanisms that regulate the differentiation towards osteoblasts and chondrocytes. Furthermore, it is known that environmental factors also influence the differentiation and control the expression of these mechanisms [7], so it is at this point where Tissue Engineering and biomaterials, as well as the specific means of differentiation used, are key issues.

Articular cartilage injury and degeneration, as well as related arthritis, are among the primary causes of disability globally. For more than 20 years, cartilage tissue engineering has been studied as a therapy option for cartilage abnormalities. Various scaffold materials have been developed for this purpose, but none have yet proven to be feasible and useful in clinical practice [8]. In the particular event of cartilage degeneration, this tissue is difficult to repair due to its avascular nature and limited self-repair capacity [9]. It is known that ASCs have the capacity to differentiate into chondrogenic cells that are characterized because they eventually form an extracellular matrix and express markers such as collagen type II and glycosaminoglycan (GAG)-chained aggrecan and hyaluronic acid [10] [–] [12]. Consequently, the regeneration of cartilage defects is typically addressed by Tissue Engineering strategies that combine BMSCs with biodegradable scaffolds [13]. However, under the influence of growth factors, ASCs have been found to undergo chondrogenic differentiation *in vitro* which could help cartilage engineering [14].

The use of MSCs in Regenerative Medicine and Tissue Engineering requires optimal growing conditions and biocompatible scaffolds, such as three-dimensional fibers produced by electrospinning. Polymer electrospinning is the most widely used technique for nanofiber manufacture, providing physical and chemical characteristics which promote growth and cell proliferation thanks to the porosity and complexity of their reticular structure, also easing cell adhesion to biomaterial surface [15,16]. Recently, in the field of musculoskeletal Tissue Engineering, nanofibrous scaffolds produced by electrospinning have become increasingly popular [17]. Electrospun nanofibrous membranes are obtained from biocompatible and usually biodegradable polymers, have a high porosity and high surface/volume ratio, and are able to mimic the structure of the extracellular matrix (ECM) [18]. The electrospinning technique is simple and versatile, allows processing a wide range of polymer materials and the resulting electrospun nanofibers are cost-effective and suitable for a variety of cellular functions [19]. Electrospun nanofibers have diameters ranging from tens to hundreds of nanometers, as collagen fibers in natural ECM [20]. For cartilage engineering, different types of polymer matrices, such as polylactic acid (PLA), polyglycolic acid (PGA), polycaprolactone (PCL), collagen type I and acellular cartilage ones have been successfully proposed [6,14].

Particularly, PLA and PCL have been shown to be ideal for nanofiber preparation in various biomedical applications, due to characteristics such as biodegradability and their ability to promote the cell growth, similar to native tissues and they can partially mimic the topographical features of the natural extracellular matrix [21,22]. PCL is a biodegradable aliphatic polyester commonly used as Tissue Engineering scaffold, which has become a promising biomaterial since it shows good mechanical resistance [23], is biocompatible, slowly degradable, non-toxic and its effectiveness promoted its approval by the FDA for use in Biomedicine. It is a bioresorbable material, compatible with soft and hard tissues [24] and is also considered a potential biomaterial for the growth and differentiation of osteoblastic and chondroblastic cells, as other authors have already shown [25]. On the other hand, PLA is a biodegradable and biocompatible aliphatic polyester, which use in different biomedical applications has also been approved by the FDA and is widely used in surgery, orthopaedics, orthodontics, traumatology and other branches of medicine [26,27]. Due to these facts, other authors have already determined its efficacy in Tissue Engineering as a scaffold intended for the growth and differentiation of mesenchymal stem cells for obtaining different cell lineages [28,29]. It has also been proved that these materials, or variations thereof, by themselves, provide an environment conducive to differentiation, without using specific factors or differentiation culture medium [30,31]. This constitutes a major progress when used in Biomedicine applications, since it would be easier to obtain new cells of interest at a lower cost and complexity when culturing cells in/on them.

While both PCL and PLA are linear aliphatic polyesters, they are different in terms of molecular structure. Thus, PCL is a more robust, hydrophobic, and crystalline polymer with a slower degradation kinetics than PLA. Conversely, PLA is stiffer and tougher than PCL [32]. When PLA and PCL are blended, the advantages of both polymers can be retained, while their drawbacks can partially be reversed [33]. Electrospun PLA/PCL blends have shown shorter degradation times and higher mechanical properties than PCL scaffolds, and additionally, bioactivity has improved. However, blends of these homopolymers have not been so widely studied as its copolymer, P(LA-co-CL), due to the immiscibility between PCL and PLA [34]. The use of both homopolymers and its blends give us the chance to tailor the evolution of the structural integrity of the scaffold throughout its material degradation.

In this context, the aim of this work is to study the bioactive properties of ASCs when grown on electrospun membranes of homopolymers of PLA and PCL and their blend (PLA/PCL). We hypothesized that PLA/PCL membranes could induce ASCs chondrogenic differentiation without a specific differentiation medium, by a synergistic effect of their chemical composition and microarchitecture. That's why the two homopolymers are compared, as membranes with analogous fiber morphology. The results forthcoming are expected to be useful in further studies in cartilage Tissue Engineering, where these cells are of great interest, but can also find other potential applications where these flat structures may mimic the damaged tissue.

2. Materials and methods

2.1. Fabrication of PLA and PCL nanofibrous scaffolds

2.1.1. Polymer solutions

Polylactic acid (PLA, INGEO 4042D, Natureworks®) and polycaprolactone (PCL, Mn = 70000-90000, Sigma®) were solved in mixtures of chloroform (chlor; estb. with ethanol, Scharlab®) and methanol (met; Scharlab®), while the blend (PLA/PCL) was solved in a mixture of dichloromethane (DCM; estb. with approx. 50 ppm amylene, Scharlab®) and dimethylformamide (DMF; Scharlab®). Solution parameters leading to electrospun membranes with precise fibers of 0.8 ± 0.2 and 1.8 ± 0.2 μm in diameter (ES 0.8 μm and ES 1.8 μm, respectively) were identified in a previous work [35]. The solutions were stirred overnight at room temperature before electrospinning.

2.1.2. Electrospinning

Nanofiber membranes were fabricated by using a homemade electrospinning device. Each polymer solution was introduced in a syringe with a 24 G (0.31 mm inner diameter) needle, which was placed in a syringe pump (RS-232, model NE 1000. New Era Pump Systems, Inc.®) to be pumped through the needle into an electric field set between the needle-tip and collector, where nanofibers can be eventually collected thanks to being covered with aluminum foil. A high voltage was applied during 30 min by using an OL400W-503 voltage source (HiTek Power®) to eject the polymer solution, which causes its elongation as fibers and the simultaneous solvent evaporation. The solution parameters, together with the electrospinning (ES) conditions for each membrane layout (flow rate, voltage and distance from needle to collector), are listed in Table 1. Once the ES membranes were obtained, the coated aluminum foil was stored in a fume hood during 24 h to ensure solvent evaporation.

In parallel, films of each polymer were prepared by solvent-casting as blanks. Polymer solutions, which have the same compositions as those for ES-1.8 μm, were poured in Petri dishes and kept in a fume hood for

Table 1
Parameters of the polymer solution and the electrospinning process to obtain PLA, PCL and PLA/PCL electrospun membranes (ES) with fibers of 0.8 and 1.8 μm in diameter.

		ES 0.8 μm	ES 1.8 μm
PLA	*Polymer concentration (% w/v)*	8	15
	Solvent ratio (% v/v)	chlor:met (66.67:33.33)	
	Flow rate (ml/h)	2	
	Voltage (kV)	25	20
	Distance to collector (cm)	13	
PCL	*Polymer concentration (% w/v)*	10	15
	Solvent ratio (% v/v)	chlor:met (70:30)	chlor:met (66.67:33.33)
	Flow rate (ml/h)	2	
	Voltage (kV)	25	
	Distance to collector (cm)	13	
PLA/ PCL	*Polymer concentration (% w/v)*	12	20
	Solvent ratio (% v/v)	DCM:DMF (75:25)	
	Flow rate (ml/h)	2	
	Voltage (kV)	25	20
	Distance to collector (cm)	15	

24 h to evaporate solvents. Finally, 150 μm thick electrospun membranes and films were punched out with a diameter of 8 mm and stored in the refrigerator before characterization.

2.2. Swelling ratio (SR)

Swelling experiments were undertaken using samples with the two configurations (films and membranes) to assess their hydrophilicity. Three samples of each polymer were weighed (m_0) in a XS105DU balance (Mettler-Toledo®) and introduced in a multiwell plate with 1 ml of distilled water each. 48 h later the samples were reweighed (m_f), after gently removing excess water with paper tissue. The swelling ratio (*SR*) was determined with the following equation:

$$SR = \frac{m_f - m_0}{m_0} \cdot 100\ (\%) \tag{1}$$

To exclude any influence of the membranes' porosities, the swelling ratio in a humid atmosphere was also determined, by using a sealed chamber. Inside the chamber was placed a glass of water and maintained at 37 °C during 48 h before the assay to achieve a saturated atmosphere. After that, three samples of each polymer were dry weighed and introduced in the chamber, kept closed at room temperature. 48 h later the samples were also reweighed.

2.3. Surface tension of films

The contact angle of different liquids (water, diethylene glycol and formamide) on polymer films was measured with a contact angle equipment DATAPHYSICS OCA20 (DataPhysics Instruments®) to study their wettability. Diethylene glycol and formamide were purchased from Sigma®.

Firstly, polar ($\sigma_L{}^P$) and dispersive ($\sigma_L{}^D$) components of the surface tension of the liquids were obtained by the Owens and Wendt model [36] using poly(tetrafluoroethylene) (PTFE) as the accepted standard reference surface. Two values were necessary for this purpose: *(i)* the global surface tension of each liquid (σ_L), which was determined with the drop pendant method (5 drops, 25 μl each) and *(ii)* the contact angle of the liquid on PTFE (θ_{PTFE}) (5 replicates). By this method, the equations used were:

$$\sigma_L^D = \frac{\sigma_L^2 \cdot (\cos\theta_{PTFE} + 1)^2}{72} \tag{2}$$

$$\sigma_L^P = \sigma_L - \sigma_L^D \tag{3}$$

With the data obtained for these solvents, the surface tension of PLA, PCL and PLA/PCL films was assessed with the following equation:

$$\frac{\sigma_L(\cos\theta + 1)}{2\cdot(\sigma_L^D)^{1/2}} = (\sigma_S^P)^{1/2} \cdot \frac{(\sigma_L^P)^{1/2}}{(\sigma_L^D)^{1/2}} + (\sigma_S^D)^{1/2} \tag{4}$$

This equation combines Young's equation relating the contact angle with the interfacial tension to the Owens and Wendt one for the two contributions to the surface tension [37]. θ is the contact angle measured by dropping 25 μl of each liquid in films and waiting 10 s for its stabilization. From the linear fitting to this equation, the dispersive and polar surface tension of each polymer, $\sigma_S{}^D$ and $\sigma_S{}^P$, were obtained from the y-ordinate and the slope, respectively.

2.4. ASCs isolation and cultivation

The experimental procedures developed in this work were approved by the Medical Committee of the University Hospital of León. Written consent was obtained from all patients by the Helsinki Declaration of 1975, as revised in 2008, and were following the current Spanish and European laws (RD 53/2013 and EU Directive 2010/63/EU). Samples of adipose tissue were obtained from healthy donors during surgical procedures at the Complejo Asistencial Universitario de León (Spain).

To isolate ASCs, approximately 5 g of adipose tissue-obtained were digested in Dulbecco's Modified Eagle Medium (DMEM; Hyclone®) containing 0.075% collagenase type I (Sigma®) for 2 h at 37 °C under stirring. The resulting cell suspension was centrifuged at 1200×*g* for 10 min. After centrifugation, the supernatant was removed and the pellet obtained was resuspended in DMEM (Hyclone®) supplemented with 10% (v/v) fetal bovine serum (FBS; Hyclone®) and 1% (v/v) penicillin/streptomycin (Hyclone®) (DMEMc). Isolated cells were multiplied in monolayer in T150 flasks (Corning®) using low-glucose DMEMc at 37 °C in a humid atmosphere containing 5% CO_2.

2.5. Cell seeding and culture on PCL, PLA and PLA/PCL membranes

PCL, PLA and PLA/PCL membranes were cut into small pieces of 5 × 5 mm, and next washed with Phosphate Buffered Saline (PBS) three times. ASCs suspensions were seeded on the PCL, PLA and PLA/PCL membranes in 24-well plates, at the rate of 1×10^5 cells per 100 μl of DMEMc. After 1 h, 1 ml of DMEMc was poured to each well and cells were incubated at 37 °C for different times depending on the experiment.

2.6. Cell viability assay

MTT [3-(4,5-dimethylthiazole-2-yl)-2,5-diphenyltetrazol bromide] assay (Invitrogen®) was performed to discard any cytotoxic effect of the different biomaterials (attributable to the solvents used for their fabrication) on the cells. Cell viability and proliferation can be determined through the MTT assay based on the mitochondrial functionality of the treated cells. ASCs were seeded (1×10^5) on each biomaterial in 24-well plates. Analysis was carried out after 1, 7 and 14 days of culture. At each culture time point, plates were incubated for 3 h at 37 °C with a medium containing DMEM without phenol red and 10% MTT. A solubilizing solution of DMSO-Isopropanol (1:1) (Fisher Scientific®) was then added and the medium was centrifuged for 30 min. Optical density in each well was quantified at 570 nm with a multiplate spectrophotometer reader Multiskan GO (Thermo Fisher Scientific®). All the experiments were developed using three biological and three technical replicates.

2.7. Scanning electron microscopy (SEM) observation

In order to analyze cell morphology, localization and distribution on the biomaterials all samples were observed by SEM. As a control, a sample of each cell-free biomaterial was used. ASCs were analyzed at 1,

7 and 14 days of culture. Samples were first washed with PBS for 5 min and fixed with 2.5% glutaraldehyde (Sigma®) for 15 min. Subsequently, the fixative was removed and 3 washes with PBS for 15 min each were made. Finally, cell dehydration was carried out by making passes of 30%, 50%, 70%, 90% and 100% ethanol, respectively, for 10 min each and repeating the last two. Once cells were dehydrated, the samples were introduced in a Critical Point Dryer CPD 030, Baltec, where they were washed with ethanol. Then, the dried samples were mounted on the grids and gold coating was carried out for observation in the JSM-6480 SEM (JEOL®), 16 mm working distance (WD) and 20 kV.

2.8. Cell spreading

To assess the average area occupied by cells on the biomaterials, the following cell culture protocol was followed using the Live/Dead viability cytotoxicity kit CF2 (Molecular Probes L3224®). The whole process was carried out under dark conditions. First, a working solution was prepared, which is obtained by diluting calcein AM 80 (Fisher Scientific®) in dimethylsulfoxide (DMSO; Sigma®), 2 μl of calcein +158 L DMSO. 1×10^5 cells were trypsinized, centrifuged for 10 min at 1200×*g* and resuspended in DMEM. Subsequently, 2 μl of calcein AM were added for each ml of the resuspended medium. Cells were incubated for 20 min in the dark at room temperature and centrifuged, and the resulting pellet was resuspended in DMEM.

60 μl of this cell-containing medium were seeded on each biomaterial and left in incubation for 1 h at 37 °C to promote cell adhesion. Subsequently, samples were washed twice with PBS and placed on a coverslip to analyze their fluorescence with a Nikon® D1 confocal microscope equipped with 3 lasers, transmission light and EZ-C1 3.70 software®. Images of fluorescent cells obtained were used to estimate the cell area occupied and the total number of cells on each sample using the NIH Image J Software®.

2.9. Cellular adhesion

The immunohistochemical technique of phalloidin staining was used to determine cell adhesion to the biomaterials. This compound prevents depolymerization of actin filaments, impeding cell movement and stabilizing the microfilaments by inhibiting the ATP-hydrolase activity of actin F. This way, when staining actin, the number of cells adhered to a certain material can be determined, since the aggregation of actin is directly proportional to the number of cells adhered to it.

The first step was to wash the samples with PBS twice for 5 min each and next fixed with 2% paraformaldehyde (Sigma®) for 15 min. PBS washings were repeated for 10 min and cells were next permeabilized with 0.1% TritonX-100 (Fisher Scientific®) solution for 30 min at room temperature. Subsequently, 3 PBS washings were repeated for 5 min each. Samples were then stained with 300 μl of Phalloidin-Tetramethylrhodamine B Isothiocyanate (TRITC; Sigma®) per sample for 40 min at room temperature and in the dark. 5 min PBS washes were carried out and finally all samples were stained with DAPI (0.2 μl of DAPI in 299.8 μl of PBS per sample) for 3 min at room temperature and in the dark. Samples were observed under a Zeiss® confocal microscope.

2.10. Immunohistochemistry

In order to evaluate the chondrogenic differentiation of ASCs proliferated on the biomaterials, immunofluorescence staining was carried out to reveal cartilage specific markers such as collagen type II and aggrecan. ASCs were seeded at 1×10^5 cells/sample in 2 Lab-tek chambers (Thermo Fisher Scientific®). ASCs were maintained in DMEMc for 21 days, with a media change every 3 days.

To follow the immunohistochemistry protocol, cells were incubated with mouse anti-human type II collagen monoclonal antibody (1:100) (Abcam®), and rabbit anti-human brevican/aggrecan polyclonal antibody (1:100) (Bioss®) overnight at 4 °C. Next, samples were incubated with secondary biotin goat anti-rabbit IgG (1:100) (Invitrogen®). They were then stained with streptavidin-Alexa 488 and streptavidin Alexa-568 antibodies (1:400) (Invitrogen®). Finally, cells in chamber slides were stained with DAPI and examined under a fluorescence microscope (Zeiss®). The "Image Analysis" module for ZEN Blue (Zeiss®) was used to analyze and quantify the fluorescence produced by each sample.

2.11. Quantitative real time PCR (qPCR)

After 21 days in culture, chondrogenic gene expression of ASCs seeded on biomaterials was analyzed by qPCR. Samples were washed with PBS and stored at −80 °C. Total RNA was extracted using the GeneMatrix Universal RNA Purification Kit (EurX®). Reverse transcription was accomplished on 1 μg of total RNA using MultiScribe® RT (Applied Biosystems®) following manufacturer's instructions of High Capacity cDNA Reverse Transcription Kit (Applied Biosystems®). Gene expression of collagen type II (COL2A1) and aggrecan (ACAN) were determined by qPCR. Assays were carried out using Step One Plus RT-PCR (Applied Biosystems®) in a total volume of 25 μl containing 0.7 μl DNA template, 1X SYBR Green (EURx®), 400 nM ROX and 0.30 U uracil-N-glycosylase (UNG) master mix, and 300 nM of each primer.

Relative quantification was carried out normalizing to the endogenous gene ACT-β. Primers were designed using the OLIGO7® primer design tool (Table 2) provided by Integrated DNA Technologies (Coralville®). All the experiments were developed using three biological and three technical replicates.

2.12. Statistical analysis

The results of this study are expressed as mean ± standard deviation (SD). Statistical analysis was carried out using the IBM® SPSS® Statistics 17 software. Significant differences among groups were determined using Student's T and ANOVA test followed by Tukey's post hoc analysis. Results with $p \leq 0.05$ were considered statistically significant.

3. Results and discussion

The behavior of ASCs on different biomaterials of PLA, PCL and their blend (PLA/PCL) was assessed by the introduction of the fiber diameter as a key factor, through proliferation, cell adhesion and chondrogenic differentiation assays.

3.1. Characterization of the membranes

Hydrophilicity and wettability are known to play an important role in cell adhesion and differentiation [38–40]. For this reason, the swelling ratios and contact angles (and surface tension) were determined for each acellular polymer substrate (Tables 3 and 4, respectively).

PCL in any of its layouts shows the lowest swelling ratio, as expected given its more hydrophobic molecular structure. That of the blend lies

Table 2
Primer sequences used in qPCR.

Gene	Genbank number	Sequence (5′ to 3′)
ACT-β	NM_001101.5	Forward Human ACT-β 5′-GACGACATGGAGAAAATCTG-3′ Reverse Human ACT-β 5′ATGATCTGGGTCATCTTCTC-3′
COL2A1	NM_001844.5	Forward Human COL2A1 5′-CTGCTATTGCCCTBTGCCCGGAT-3′ Reverse Human COL2A1 5′-ACACCTCCAACGTCCAGATGACC-3′
ACAN	NM_001369268.1	Forward Human ACAN 5′-CTGCCCAACTACCCGGCCAT-3′ Reverse Human ACAN 5′-TGCGCCCTGTCAAAGTCGAG-3′

Table 3
Equilibrium swelling ratio of PLA, PCL and PLA/PCL electrospun membranes with fiber diameters of 0.8 and 1.8 μm, and films as controls, in distilled water and in a saturated humid atmosphere.

	PLA	PCL	PLA/PCL
Immersed in water			
Films	11.94 ± 0.84%	2.98 ± 0.82%	4.12 ± 0.64%
ES 0.8 μm	225.4 ± 29.6%	74.3 ± 4%	172.1 ± 17.8%
ES 1.8 μm	1067.7 ± 36.1%	135.7 ± 24.2%	523.5 ± 31.3%
In a saturated humid atmosphere			
Films	1.76 ± 0.20%	0.75 ± 0.04%	1.46 ± 0.18%
ES 0.8 μm	8.19 ± 0.40%	1.87 ± 0.10%	4.23 ± 0.60%
ES 1.8 μm	8.58 ± 0.27%	1.72 ± 0.20%	4.45 ± 0.18%

Table 4
Water contact angle and surface tension of PLA, PCL and PLA/PCL films.

	PLA	PCL	PLA/PCL
θ_{water} (°)	59.46 ± 0.43	75.40 ± 0.35	66.60 ± 0.19
$\theta_{formamide}$ (°)	43.34 ± 0.40	58.62 ± 0.20	49.24 ± 0.15
$\theta_{diethylene\ glycol}$ (°)	48.84 ± 0.11	37.68 ± 0.25	44.78 ± 0.29
σ_S (mN/m)	42.98	37.31	38.71
σ_S^D (mN/m)	16.56	30.10	22.05
σ_S^P (mN/m)	26.42	7.21	16.66

between those of the homopolymers. Interestingly enough, swelling in liquid water of membranes with 1.8 μm-fiber diameter is higher than that of analogous membranes with 0.8 μm-fiber diameter: 2- and 5-fold for PCL and PLA membranes and 3-fold for their blend. Furthermore, the electrospun format allows more than 20 times more swelling in water for all membranes than in solvent cast films. This is attributed to the expansion of the membranes as three-dimensional microporous scaffolds, allowing free water to be retained in its pores. This effect is enhanced when the diameter of the fibers is greater, because the fibers fall on the collector less intertwined, allowing the membranes to expand more. Additionally, the greater affinity of PLA with water facilitates the confinement of water in these pores.

To leave out of account the free water withheld in the pores of these scaffolds, the membranes and films were in parallel swollen in a saturated humid atmosphere. In this case, the swelling of membranes is 2.3–4.9-fold that of films, not finding any difference attributed to the diameter of the fibers. This difference between membranes and films may be an indication of the interconnected inner spaces left as the solvents evaporate from the fibers, which facilitates water diffusion throughout the fibers. Furthermore, since swelling is dependent on the accessible surface for the water molecules to be absorbed by the bulk material (i.e., the effective surface area), similar values shown by different fiber diameters may indicate similar interface areas.

Water contact angles on the films of different composition, and their surface tension (σ_S), including dispersive and polar components (σ_S^D and σ_S^P), are shown in Table 4. These results agree with the swelling ratio, PCL being the least wettable biomaterial because of its most hydrocarbonated chain. Conversely, with a lower polar liquid, like diethylene glycol, the trend was reversed. The surface tension, therefore, is the lowest for PCL, its polar component representing 19.33% of it, whereas it increases up to 43.0 and 61.47% for the blend and pure PLA, respectively.

SEM images of the acellular membranes are shown in Fig. 1. They are homogeneous in all cases, without defects such as beads, for both pursued fiber diameters (0.8 and 1.8 μm), which were obtained by setting the main electrospinning parameters (polymer concentration, solvents, solvent ratio, flow rate, voltage and distance from needle to collector) for each polymer and targeted diameter. These images also allowed us to rule out any surface roughness, so that the biological behavior results can be safely correlated with the polymer nature and the fiber diameter.

3.2. ASCs culture scaffolds: morphological and bioactive characteristics on PLA/PCL membranes

In terms of fiber size, it is verified that this physical property is going to affect the cellular behavior. This is due to the fact that the bioactive properties and the interaction of the cells with different biomaterials are modified, affecting the adhesion, the proliferation and the differentiation capacity depending on the fiber diameter [41]. The control of the biomaterial characteristics is a fundamental step in its development, since different results will be obtained depending on certain parameters, characterizing it or not as a suitable candidate for cell adhesion and proliferation. Electrospun fibers feature a variety of morphological structures at the surface and in the bulk, depending on the average fiber diameter. As a result, the fiber size of electrospun materials may affect surface shape, mechanical and bioactive properties [42,43].

The effect of fiber size on cell behavior was analyzed in materials of 0.8 and 1.8 μm-fiber diameter. In Fig. 2 the proliferation of ASCs for each culture time on the different biomaterials is shown. Cells were viable when they were cultured on all the membranes according to the results obtained from the MTT assay, though the highest proliferation rate was obtained on PCL membranes with 1.8 μm-fiber diameter. In fact, it has been shown that cells proliferate faster on a less stiff substrate such as PCL membranes than on PLA ones [44]. The PLA/PCL membrane with 0.8 μm-fiber diameter presents significant differences when comparing cell proliferation on day 1 of the experiment with the rest of the 0.8 μm biomaterials on days 1 and 7, determining that it is the one with the highest cell concentration on day 1. A larger fiber diameter provides a more spacious surface for cells to adhere and allows their proper expansion. These results are consistent with those of other authors analyzing cell proliferation on PLA and PCL scaffolds, where the increase in fiber diameter was directly proportional to cell proliferation [45,46]. A smaller fiber size has been shown to hinder the cell binding to the scaffold surface and avoid establishing secure adhesion, which could also be the case here for 0.8 μm. On the other hand, the lower surface tension of the PLA/PCL blends, and even more PCL substrates, seem to facilitate cell adhesion and subsequent proliferation with respect to PLA.

Cell morphology and arrangement on each membrane was observed after 1, 7 and 14 days in culture by SEM. The morphology of ASCs seeded on PLA, PCL and their blend is shown in Fig. 3. In the case of PLA 0.8 μm a shortage of cells during the test was observed for all time points; at day 14, some isolated cells appeared onto the fibers of the biomaterial. However, on PLA fibers of greater diameter (1.8 μm), the opposite occurs: cell growth ranges from a very low cell density, to a compact monolayer after 14 days. When ASCs were seeded on the PCL membranes from the beginning of the test on day 1, until the end of the test after 14 days, a single cell layer that completely coats the fibers of the biomaterials of both diameters (0.8 μm and 1.8 μm) was observed. Nonetheless, a different cell behavior was found on PLA/PCL surfaces. On PLA/PCL 0.8 μm, a single layer of cells was observed on the first day, but cell number gradually decreased until there were hardly any cells left on the last time point. In contrast, in the 1.8 μm PLA/PCL, very few cells can be observed at day 1, while on day 14 a higher cell density is shown, although it was not a monolayer as in other cases.

To analyze the average area occupied by the cells cultured on the biomaterials and quantify the number of living cells on each one after 1 h of culture, the spreading test was followed. Results obtained are shown in Fig. 4, left. Images show a significantly higher number of cells in the case of those biomaterials with a larger diameter (1.8 μm). It can also be seen that the PCL 0.8 μm membrane has the lowest number of cells on its surface, in relation to others of the same diameter. As for the biomaterials with thicker fibers (1.8 μm), it was noticed that the number of cells adhered was very high and they were also very evenly distributed throughout the biomaterial.

In order to quantify which of the biomaterials had the largest number of cells distributed on its surface, the confocal images were analyzed with the NIH Image J Software®, which allowed the cell count of 3

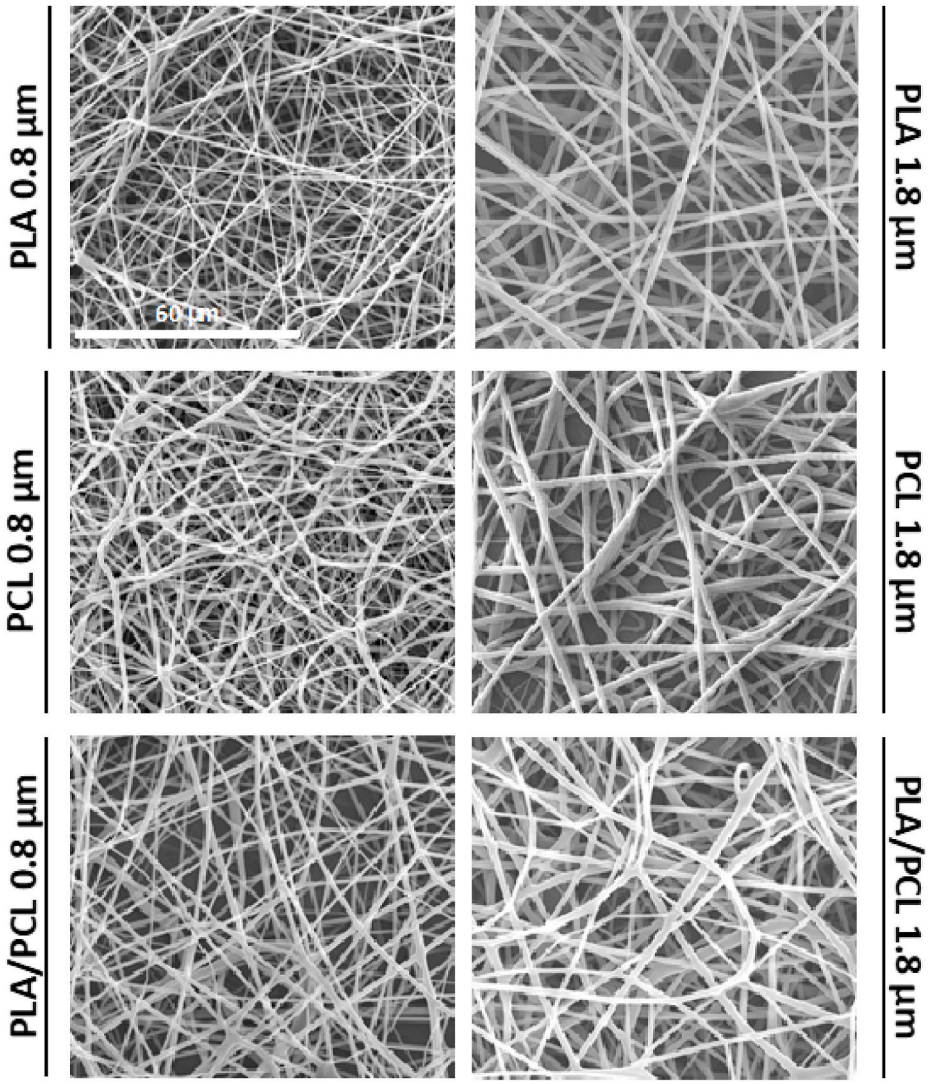

Fig. 1. SEM images of acellular electrospun membranes of PLA, PCL and PLA/PCL, with fiber diameters of 0.8 µm and 1.8 µm. All images share the same scale bar: 60 µm.

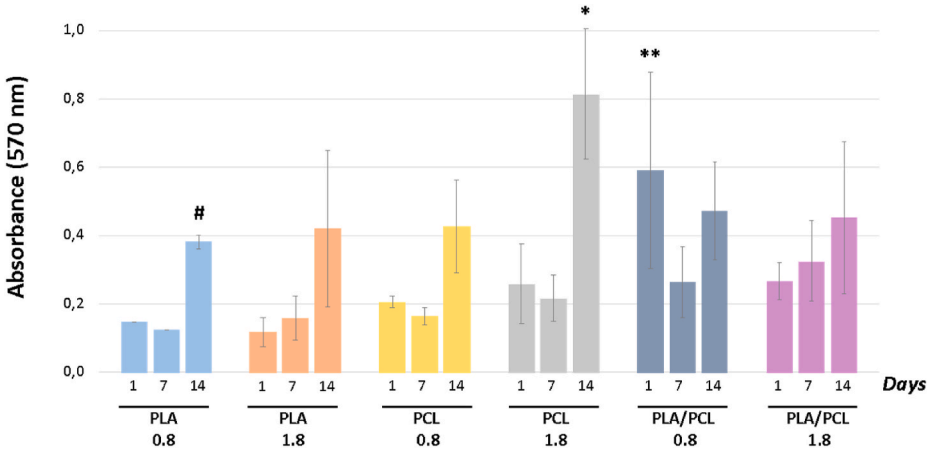

Fig. 2. MTT assay of ASCs on the electrospun membranes. The number of viable cells is expressed as the increased absorbance of the MTT test on days 1, 7 and 14 of culture (from left to right in each case). # p-value < 0.05 vs. PLA 0.8 µm days 1 and 7. Statistical differences are indicated as: * p-value < 0.05 vs. PLA 0.8 µm, PLA 1.8 µm, PCL 0.8 µm, PLA/PCL 0.8 µm days 7 and 14, PLA/PCL 1.8 µm ** p-value < 0.01 vs. PLA 0.8 µm days 1 and 7, PLA 1.8 µm days 1 and 7, PCL 0.8 µm days 1 and 7, PCL 1.8 µm days 1 and 7, PLA/PCL 1.8 µm days 1 and 7. N = 3.

biological replicates of each biomaterial after 1 h of culture (Fig. 4, right). Results obtained were represented graphically in order to see the differences found between the biomaterials. The 1.8 µm-fiber diameter PCL ($p = 0.034$) and the 1.8 µm PLA/PCL ($p = 0.017$) showed substantial differences compared to the rest of the biomaterials. However, significant differences were also seen between them: a much higher number of cells was found in 1.8 µm PLA/PCL. On the other hand, as regards to the rest of the biomaterials, no differences were found

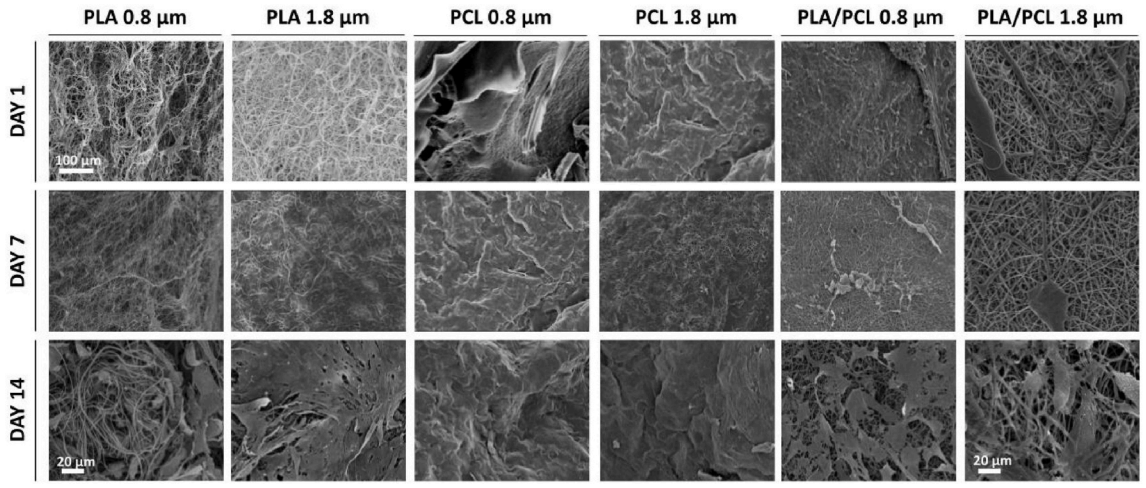

Fig. 3. SEM images of electrospun membranes cultured with ASCs on PLA, PCL and their blend membranes (by columns) having fiber diameters of 0.8 and 1.8 µm, on days 1, 7 and 14 of culture (x220). All the images share the same scale bar: 100 µm (except images with another scale bar in the bottom row).

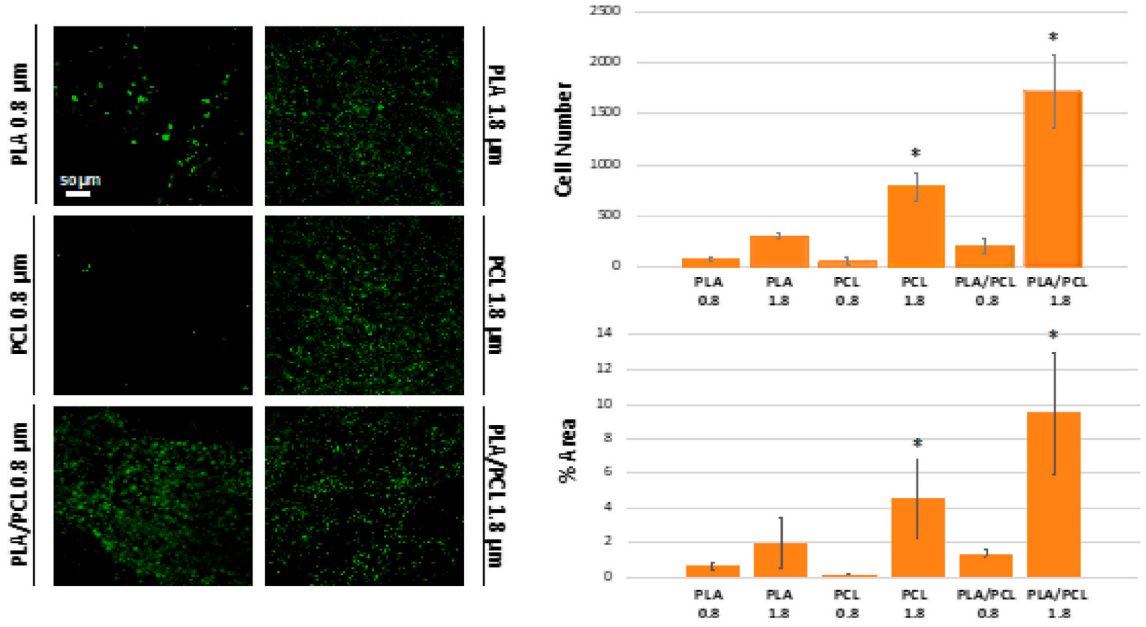

Fig. 4. Left: LIVE/DEAD staining of ASCs seeded on each material and cultured for 1 h. The green fluorescence represents the living cells. Scale bar: 50 µm. Top-right: Number of living cells after 1 h quantified using the spreading assay. Statistical differences are indicated as: * p-value < 0.05 vs. PLA 0.8 µm, PLA 1.8 µm, PCL 0.8 µm and PLA/PCL 0.8 µm. Bottom-right: Percentage of area occupied by cells in the center area of each biomaterial. * p-value < 0.05 vs. PLA 0.8 µm, PLA 1.8 µm, PCL 0.8 µm and PLA/PCL 0.8 µm. (For interpretation of the references to colour in this figure legend, the reader is referred to the Web version of this article.)

between them, so 0.8 µm and 1.8 µm PLA can be considered almost equivalent in terms of cells found on their surface and the percentage of cell area used. In summary, best results in cell spreading assay were obtained in all 1.8 µm membranes mainly when PLA/PCL 1.8 µm was used. The addition of PLA into a PCL nanofibrous matrix clearly enhances cell spreading, likely due to the higher hydrophilic characteristics of PLA, which allows a more favorable three-dimensional cell environment. These results point out to a synergistic effect of the surface tension of these polyesters, together with that of the fiber diameter.

Regarding the analysis of cell adhesion to the membranes, ASCs were stained with phalloidin after 1 day of culture (Fig. 5). Fluorescence of each sample was quantified using the NIH Image J Software®. Cell adhesion was much higher and more evenly distributed on the PCL membranes with a fiber diameter of 1.8 µm. In the rest of the biomaterials there were very few cells adhered and with a very heterogeneous distribution. Although adhesion results obtained in PLA/PCL blends were significantly higher than on PLA and PCL of 0.8 µm, the best adhesion values were obtained unquestionably on PCL of 1.8 µm.

Although the hydrophobicity of pure PCL makes in principle its scaffold adverse to cell adhesion, growth and differentiation [47], this aspect is improved when the fiber size is increased or PCL is combined with PLA as blend [48]. Although PLA has successful applications as a biomaterial in Tissue Engineering, some authors have described the lack of functional groups that promote adhesion to its surface [21]. In agreement with these results, this study shows that the proliferation and adhesion of ASCs increases when PCL is blended with PLA in comparison with pure PLA. In membranes with smaller fiber diameter, PLA/PCL blends improved slightly cell adhesion compared to PLA and PCL, but did not improve the results of adhesion and proliferation obtained with PCL with a greater diameter. In some point results obtained of cell adhesion and proliferation seem to be contradictory. However, early steps of cell adhesion include cell contact, attachment, and subsequent

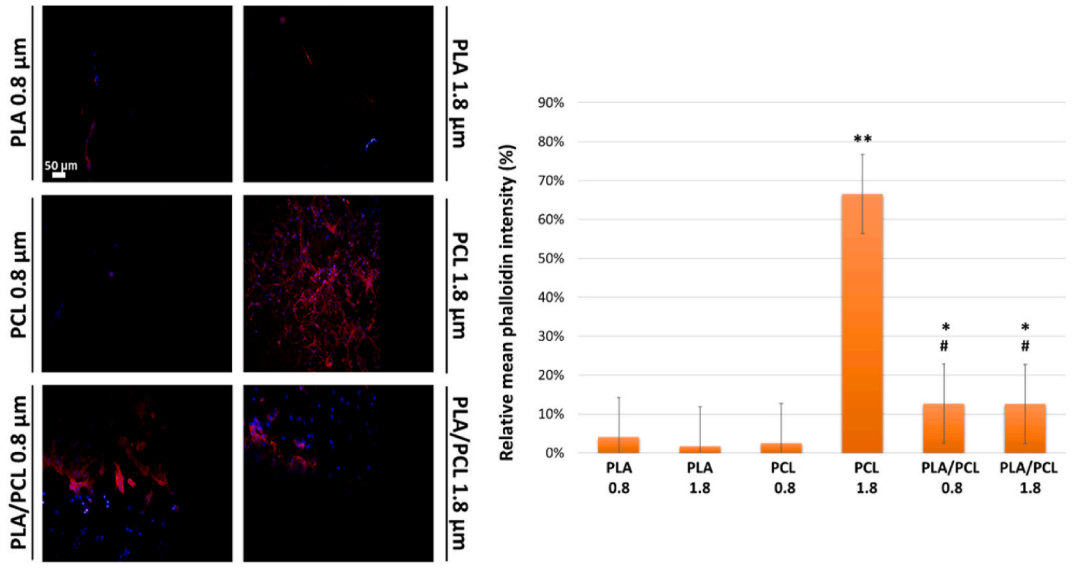

Fig. 5. Cellular adhesion. Left: Confocal images of cellular adhesion. All images share the same scale bar: 50 µm. Right: Quantification of fluorescence on each biomaterial. Statistical differences are indicated as: * p-value < 0.05 vs. PLA 0.8 µm $^{\#}$ p-value < 0.01 vs. PLA 1.8 µm and PCL 0.8 µm ** p-value < 0.01 vs PLA 0.8 µm, PLA 1.8 µm and PCL 0.8 µm PCL.

adherence of anchorage-dependent cells. Filopodia extension is thought to be the first point of interaction between the cell and the substratum. Filopodia firmly connect to the substrate and play a key function in directing cells on the surface as well as starting the process of modifying the substratum for better cell adhesion. Physical forces dominate the early attachment phase, which is devoid of considerable extracellular matrix (ECM) formation. Cells connected to a surface spread slowly (usually within hours) over the surface, exhibiting a strong "biological component of adhesion" that includes ECM secretion and results in the flattening of cells on the substratum, depending on compatibility with the surface. The amount of time it takes to complete contact and attachment phases is determined by a complicated interaction between the cell and the biomaterial surface [49].

3.2.1. PLA/PCL membranes induce ASCs chondrogenic differentiation

Regarding ASCs chondrogenic differentiation, it was positive in cultures on all biomaterials. This means that these membranes, with their respective variations in fiber diameter, provide a favorable environment for differentiation without the addition of specific factors or differentiation culture medium. It has been already observed that the diameter of PLA fibers used as scaffolds had a key role in the support and chondrogenic differentiation of mesenchymal stem cells [50,51] and cells in 3D culture react differently depending on the fiber size [22].

Chondrogenic differentiation was confirmed by analyzing COL2A1 and ACAN genes using qPCR and confocal microscopy. COL2A1 and ACAN are specific markers of cartilage differentiation. Best results for the expression of the COL2A1 gene, confirmed using immunofluorescence, were obtained in PLA of 1.8 µm and in PLA/PCL for both fiber diameter (Fig. 6). In previous works, it has already been proved that in

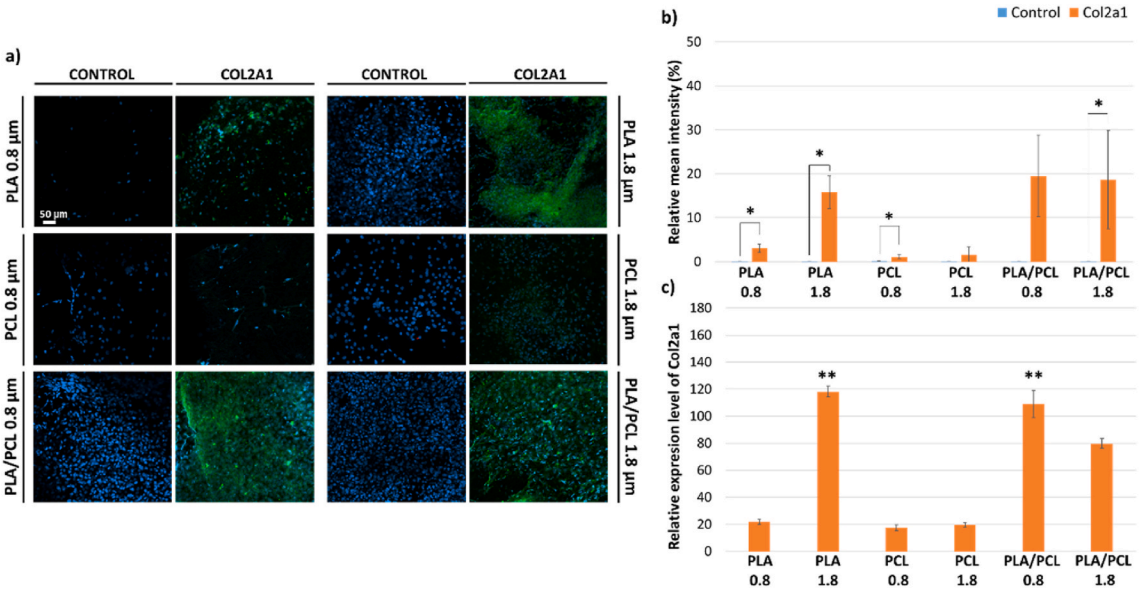

Fig. 6. Collagen type II expression. a) Confocal microscopy images of collagen type II. ASCs cultured for 21 days. All images share the same scale bar: 50 µm. b) Quantification of fluorescence on each biomaterial. Statistical differences are indicated as * p-value < 0.05. c) Gene expression of Collagen type II (COL2A1) after 21 days in culture. Statistical differences are indicated as **p < 0.01 versus PLA 0.8 µm, PCL 0.8 µm and PCL 1.8 µm.

PLA biomaterials it is possible to induce differentiation with stem cells derived from adipose tissue [52]. On PLA membranes, after 21 days of culture, ASCs could develop more cell-cell interactions, which play an important role in chondrocytes differentiation and phenotype expression [53]. Furthermore, in this case, the fiber diameter of the scaffolds significantly affects the ability of differentiation. These results agree with other authors, who obtained better results for the expression of the COL2A1 gene in scaffolds composed of microfibers than in others with nanometer scale components [54]. A microfiber, which provides a more spacious surface than a nanofiber, plays key roles in cell signaling, differentiation, intracellular transport, cell-matrix interactions and other cellular events [55]. As for PCL membranes, chondrogenic differentiation was weaker in any of its formats (1.8 μm and 0.8 μm) as compared to PLA or the blend.

Finally, concerning results obtained for the chondrogenic differentiation evaluating ACAN gene, the combination of PLA/PCL for 1.8 μm fiber diameter was the best option (Fig. 7). Positive results have also been shown in differentiation processes with scaffolds that had a weight ratio of 1/1 in PCL and PLA [56], but in this case the size of the fiber did not affect the differentiation capacity. The combination of both polymeric materials with opposite characteristics results in a more efficient chondrogenic differentiation for ACAN gene than that of any of its homopolymers, independently of fiber size.

To sum up, positive fluorescence was obtained for COL2A1 and ACAN on all membranes. An enhanced chondrogenesis on PLA of 1.8 μm and PLA/PCL blends of both fiber diameters was confirmed using confocal microscopy. A weaker gene expression of both genes was found when ASCs were cultured on PLA of 0.8 μm and PCL biomaterials. These results are in line with the work of other authors [31] and imply numerous advantages over the limitations offered by the use of specific factors, such as growth and differentiation factors. Their half-life is too short to ensure *in vivo* efficacy, a single administration is usually not enough to attain an adequate biological effect, the quantities required are prohibitively expensive, and continuous protein production increases the likelihood of undesired outcomes [57]. Moreover, a recent report has described that biochemical (growth factors supplementation) and physical (nanofiber) cues regulated similar ontological pathways, suggesting an overlap in the molecular mechanisms that these stimuli use to control stem cell function [58]. Other authors have demonstrated that the diameter of PLA fibers used as scaffolds has an influential role in the support and chondrogenic differentiation of mesenchymal stem cells [59]. Although pure PCL hydrophobicity makes the scaffold adverse to cell adhesion, growth and differentiation [60], our *in vitro* cell differentiation results showed that electrospun PCL scaffolds were favorable for chondrogenic differentiation, possibly due to PCL is soft, elastic and show a relatively low stiffness/modulus due to its rubber behavior at 37 °C as a consequence of a glass transition temperature well below the cell culture temperature [32,35]. These characteristics are able to promote the chondrogenic differentiation through mimicking the physiological cartilage formation [61].

4. Conclusions and outlook

Both the composition and microstructure of polymeric biomaterials are crucial in terms of cell interaction, and slight adjustments, in particular of the surface tension and fiber diameter, may result in better or worse candidates for cell adhesion, proliferation and differentiation. Depending on the parameter assessed, different results were obtained on each biomaterial. Using polylactic acid (PLA) and polycaprolactone (PCL) as fibrous cell supports with fiber diameter of 0.8 and 1.8 μm, successful results in terms of ASCs viability were obtained, although in the case of PCL the cellular response was significantly better. Positive outcomes were also attained when blending both polyesters (PLA/PCL) but the blend did not seem to overtake the outstanding biological performance of PCL in neither of the membrane configurations. Best results for both cell adhesion and differentiation were obtained using these biomaterials with a larger fiber diameter (1.8 μm *vs.* 0.8 μm). Particularly, the use of PCL would be more convenient for cell adhesion, whereas PLA or PCL/PLA blends would be more appropriate for cell differentiation. In addition, this study has shown the capacity of ASCs to differentiate into chondrocytes without the need for the addition of any differentiation medium. Regarding the combination of both polymers, more studies would be required to evaluate their properties and finally tune the best proportion between them for a specific experiment, and control these features will be key in cartilage Tissue Engineering development.

Author contributions

V.V., A.V, J. R and G.V conceived and planned the experiments. M.H,

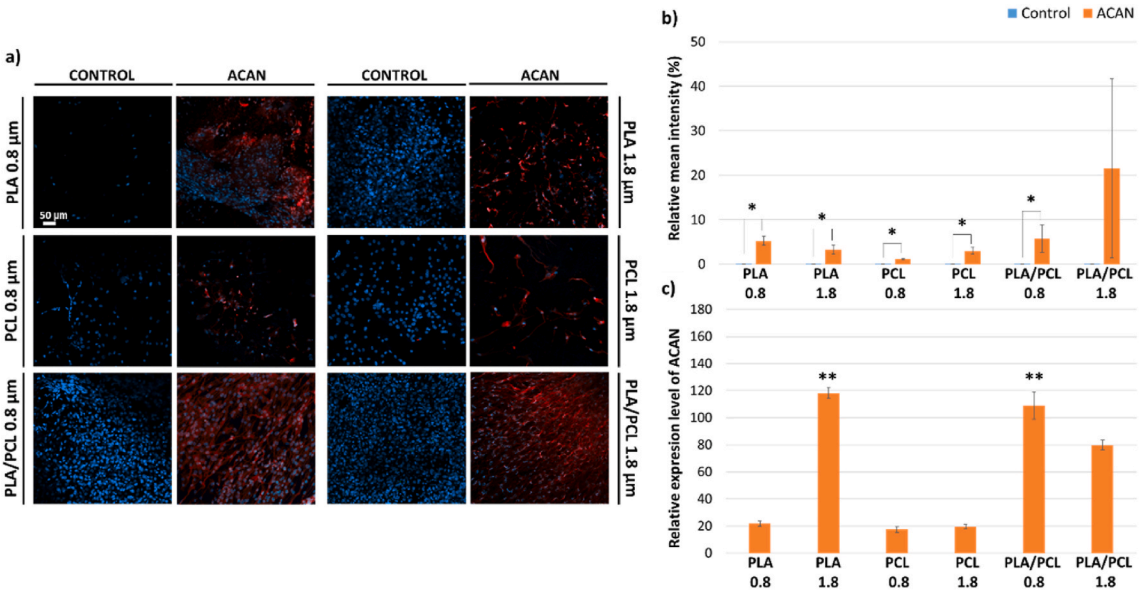

Fig. 7. Aggrecan expression. a) Confocal microscopy images of aggrecan. ASCs cultured for 21 days. Scale bar: 50 μm. b) Quantification of fluorescence on each biomaterial. Statistical differences are indicated as * p-value < 0.05. c) Gene expression of aggrecan (ACAN) after 21 days in culture. Statistical differences are indicated as **$p < 0.01$ versus PLA 0.8, PCL 0.8 μm and PCL 1.8 μm.

S.A. and M.G. carried out the experiments. J.R and G.V. contributed to sample preparation. M.H, S.A., M.G., J.R, G.V., A.V and V.V. contributed to the interpretation of the results. A.V. and V.V. took the lead in writing the manuscript. All authors provided critical feedback and helped shape the research, analysis and supervised the manuscript.

Data availability statement

The data that support the findings of this study are available from the corresponding author, upon reasonable request.

Funding statement

This study was financially supported by the Spanish Ministerio de Economía y Competitividad through the BES-2016-078024 grant.

Declaration of competing interest

The authors declare that they have no known competing financial interests or personal relationships that could have appeared to influence the work reported in this paper.

Acknowledgments

We are very grateful to Aroa Vicente Puertas and Sara Herrero for their technical support.

References

[1] A.S. Mao, D.J. Mooney, Regenerative medicine: current therapies and future directions, Proc. Natl. Acad. Sci. U.S.A. 112 (2015) 14452–14459, https://doi.org/10.1073/pnas.1508520112.
[2] C.M. Nelson, M.J. Bissell, Of extracellular matrix, scaffolds, and signaling: tissue architecture regulates development, homeostasis, and cancer, Annu. Rev. Cell Dev. Biol. 22 (2006) 287–309, https://doi.org/10.1146/annurev.cellbio.22.010305.104315.
[3] A. Jaklenec, A. Stamp, E. Deweerd, A. Sherwin, R. Langer, Progress in the tissue engineering and stem cell industry “are we there yet? Tissue Eng. B Rev. 18 (2012) 155–166, https://doi.org/10.1089/ten.teb.2011.0553.
[4] A. Bongso, M. Richards, History and perspective of stem cell research, Best Pract. Res. Clin. Obstet. Gynaecol. 18 (2004) 827–842, https://doi.org/10.1016/j.bpobgyn.2004.09.002.
[5] G. Donofrio, A. Capocefalo, V. Franceschi, G. Morini, M. Del Bue, V. Conti, S. Cavirani, S. Grolli, Virally and physically transgenized equine adipose-derived stromal cells as a cargo for paracrine secreted factors, BMC Cell Biol. 11 (2010), https://doi.org/10.1186/1471-2121-11-73.
[6] S. Pérez-Castrillo, M.L. González-Fernández, M.E. López-González, V. Villar-Suárez, Effect of ascorbic and chondrogenic derived decellularized extracellular matrix from mesenchymal stem cells on their proliferation, viability and differentiation, Ann. Anat. 220 (2018) 60–69, https://doi.org/10.1016/j.aanat.2018.07.006.
[7] D.J. Kelly, C.R. Jacobs, The role of mechanical signals in regulating chondrogenesis and osteogenesis of mesenchymal stem cells, Birth Defects Res. Part C Embryo Today - Rev. 90 (2010) 75–85, https://doi.org/10.1002/bdrc.20173.
[8] S.L. Brennan-Olsen, S. Cook, M.T. Leech, S.J. Bowe, P. Kowal, N. Naidoo, I. N. Ackerman, R.S. Page, S.M. Hosking, J.A. Pasco, M. Mohebbi, Prevalence of arthritis according to age, sex an[1] Brennan-Olsen SL, Cook S, Leech MT, Bowe SJ, Kowal P, Naidoo N, et al. Prevalence of arthritis according to age, sex and socioeconomic status in six low and middle income countries: analysis of data from, BMC Muscoskel. Disord. 18 (2017), https://doi.org/10.1186/S12891-017-1624-Z.
[9] A. Lindahl, M. Brittberg, L. Peterson, Lohmander Grodzinsky, Caplan Buschman, Cartilage repair with chondrocytes: clinical and cellular aspects, Novartis Found. Symp. 249 (2003) 175–189, https://doi.org/10.1002/0470867973.ch13.
[10] P.A. Zuk, M. Zhu, P. Ashjian, D.A. De Ugarte, J.I. Huang, H. Mizuno, Z.C. Alfonso, J.K. Fraser, P. Benhaim, M.H. Hedrick, Human adipose tissue is a source of multipotent stem cells, Mol. Biol. Cell 13 (2002) 4279–4295, https://doi.org/10.1091/mbc.E02-02-0105.
[11] P.A. Zuk, M. Zhu, H. Mizuno, J. Huang, J.W. Futrell, A.J. Katz, P. Benhaim, H. P. Lorenz, M.H. Hedrick, Multilineage cells from human adipose tissue: implications for cell-based therapies, Tissue Eng. 7 (2001) 211–228, https://doi.org/10.1089/107632701300062859.
[12] T. Aigner, J. Stöve, Collagens - major component of the physiological cartilage matrix, major target of cartilage degeneration, major tool in cartilage repair, Adv. Drug Deliv. Rev. 55 (2003) 1569–1593, https://doi.org/10.1016/j.addr.2003.08.009.
[13] G. Zhou, W. Liu, L. Cui, X. Wang, T. Liu, Y. Cao, Repair of porcine articular osteochondral defects in non-weightbearing areas with autologous bone marrow stromal cells, Tissue Eng. 12 (2006) 3209–3221, https://doi.org/10.1089/ten.2006.12.3209.
[14] U. Nöth, L. Rackwitz, A. Heymer, M. Weber, B. Baumann, A. Steinert, N. Schütze, F. Jakob, J. Eulert, Chondrogenic differentiation of human mesenchymal stem cells in collagen type I hydrogels, J. Biomed. Mater. Res. 83 (2007) 626–635, https://doi.org/10.1002/jbm.a.31254.
[15] E. Curcio, A. Piscioneri, S. Morelli, S. Salerno, P. Macchiarini, L. De Bartolo, Kinetics of oxygen uptake by cells potentially used in a tissue engineered trachea, Biomaterials 35 (2014) 6829–6837, https://doi.org/10.1016/j.biomaterials.2014.04.100.
[16] E. Curcio, P. Macchiarini, L. De Bartolo, Oxygen mass transfer in a human tissue-engineered trachea, Biomaterials 31 (2010) 5131–5136, https://doi.org/10.1016/j.biomaterials.2010.03.013.
[17] J. Cai, J. Wang, K. Ye, D. Li, C. Ai, D. Sheng, W. Jin, X. Liu, Y. Zhi, J. Jiang, J. Chen, X. Mo, S. Chen, Dual-layer aligned-random nanofibrous scaffolds for improving gradient microstructure of tendon-to-bone healing in a rabbit extra-articular model, Int. J. Nanomed. 13 (2018) 3481–3492, https://doi.org/10.2147/IJN.S165633.
[18] Q. Yang, J. Peng, Q. Guo, J. Huang, L. Zhang, J. Yao, F. Yang, S. Wang, W. Xu, A. Wang, S. Lu, A cartilage ECM-derived 3-D porous acellular matrix scaffold for in vivo cartilage tissue engineering with PKH26-labeled chondrogenic bone marrow-derived mesenchymal stem cells, Biomaterials 29 (2008) 2378–2387, https://doi.org/10.1016/j.biomaterials.2008.01.037.
[19] X. Wang, B. Ding, B. Li, Biomimetic electrospun nanofibrous structures for tissue engineering, Mater. Today 16 (2013) 229–241, https://doi.org/10.1016/j.mattod.2013.06.005.
[20] J. Wang, C.M. Valmikinathan, W. Liu, C.T. Laurencin, X. Yu, Spiral-structured, nanofibrous, 3D scaffolds for bone tissue engineering, J. Biomed. Mater. Res. 93 (2010) 753–762, https://doi.org/10.1002/jbm.a.32591.
[21] T. Matsui, Y. Arima, N. Takemoto, H. Iwata, Cell patterning on polylactic acid through surface-tethered oligonucleotides, Acta Biomater. 13 (2015) 32–41, https://doi.org/10.1016/j.actbio.2014.11.011.
[22] G.T. Christopherson, H. Song, H.Q. Mao, The influence of fiber diameter of electrospun substrates on neural stem cell differentiation and proliferation, Biomaterials 30 (2009) 556–564, https://doi.org/10.1016/j.biomaterials.2008.10.004.
[23] M.A. Woodruff, D.W. Hutmacher, The return of a forgotten polymer - polycaprolactone in the 21st century, Prog. Polym. Sci. 35 (2010) 1217–1256, https://doi.org/10.1016/j.progpolymsci.2010.04.002.
[24] H.L. Khor, K.W. Ng, A.S. Htay, J.-T. Schantz, S.H. Teoh, D.W. Hutmacher, Preliminary study of a polycaprolactone membrane utilized as epidermal substrate, J. Mater. Sci. Mater. Med. 14 (2003) 113–120, https://doi.org/10.1023/a:1022059511261.
[25] D.W. Hutmacher, T. Schantz, I. Zein, K.W. Ng, S.H. Teoh, K.C. Tan, Mechanical properties and cell cultural response of polycaprolactone scaffolds designed and fabricated via fused deposition modeling, J. Biomed. Mater. Res. 55 (2001) 203–216, https://doi.org/10.1002/1097-4636(200105)55:2<203::AID-JBM1007>3.0.CO, 2-7.
[26] L.T. Lim, R. Auras, M. Rubino, Processing technologies for poly(lactic acid), Prog. Polym. Sci. 33 (2008) 820–852, https://doi.org/10.1016/j.progpolymsci.2008.05.004.
[27] I.S.M.A. Tawakkal, M.J. Cran, J. Miltz, S.W. Bigger, A review of poly(lactic acid)-based materials for antimicrobial packaging, J. Food Sci. 79 (2014) R1477–R1490, https://doi.org/10.1111/1750-3841.12534.
[28] J.M. Moran, D. Pazzano, L.J. Bonassar, Characterization of polylactic acid-polyglycolic acid composites for cartilage tissue engineering, Tissue Eng. 9 (2003) 63–70, https://doi.org/10.1089/107632703762687546.
[29] J.S. Wayne, C.L. McDowell, K.J. Shields, R.S. Tuan, In vivo response of polylactic acid-alginate scaffolds and bone marrow-derived cells for cartilage tissue engineering. Tissue Eng., 2005, pp. 953–963, https://doi.org/10.1089/ten.2005.11.953.
[30] M. Alves da Silva, A. Martins, A.R. Costa-Pinto, N. Monteiro, S. Faria, R.L. Reis, N. M. Neves, Electrospun nanofibrous meshes cultured with wharton’s jelly stem cell: an alternative for cartilage regeneration, without the need of growth factors, Biotechnol. J. 12 (2017), https://doi.org/10.1002/biot.201700073.
[31] R. Moradian Tehrani, H. Mirzaei, J. Verdi, A. Sahebkar, M. Noureddini, R. Salehi, B. Alani, M. Kianmehr, Chondrogenic differentiation of human scalp adipose-derived stem cells in Polycaprolactone scaffold and using Freeze Thaw Freeze method, J. Cell. Physiol. 233 (2018) 6705–6713, https://doi.org/10.1002/jcp.26477.
[32] J.C. Middleton, A.J. Tipton, Synthetic biodegradable polymers as orthopedic devices, Biomaterials 21 (2000) 2335–2346, https://doi.org/10.1016/S0142-9612(00)00101-0.
[33] G. Zhang, G.L. Fiore, T.L.S. Clair, C.L. Fraser, Difluoroboron dibenzoylmethane pcl-pla block copolymers: matrix effects on room temperature phosphorescence, Macromolecules 42 (2009) 3162–3169, https://doi.org/10.1021/ma9000622.
[34] Q. Yao, J.G.L. Cosme, T. Xu, J.M. Miszuk, P.H.S. Picciani, H. Fong, H. Sun, Three dimensional electrospun PCL/PLA blend nanofibrous scaffolds with significantly improved stem cells osteogenic differentiation and cranial bone formation, Biomaterials 115 (2017) 115–127, https://doi.org/10.1016/j.biomaterials.2016.11.018.
[35] M. Herrero-Herrero, J.A. Gómez-Tejedor, A. Vallés-Lluch, PLA/PCL electrospun membranes of tailored fibres diameter as drug delivery systems, Eur. Polym. J. 99 (2018) 445–455, https://doi.org/10.1016/j.eurpolymj.2017.12.045.

[36] D.K. Owens, R.C. Wendt, Estimation of the surface free energy of polymers, J. Appl. Polym. Sci. 13 (1969) 1741–1747, https://doi.org/10.1002/APP.1969.070130815.
[37] A.W. Neumann, R. David, Y. Zuo, Applied Surface Thermodynamics, 2011.
[38] M.S. Godbole, A. Seyda, J. Kohn, T.L. Arinzeh, Surface properties of the substratum affect human mesenchymal stem cell differentiation, Proc. IEEE Annu. Northeast Bioeng. Conf. NEBEC. 30 (2004) 116–117, https://doi.org/10.1109/NEBC.2004.1300020.
[39] B. Valamehr, S.J. Jonas, J. Polleux, R. Qiao, S. Guo, E.H. Gschweng, B. Stiles, K. Kam, T.J.M. Luo, O.N. Witte, X. Liu, B. Dunn, H. Wu, Hydrophobic surfaces for enhanced differentiation of embryonic stem cell-derived embryoid bodies, Proc. Natl. Acad. Sci. U.S.A. 105 (2008) 14459–14464, https://doi.org/10.1073/PNAS.0807235105.
[40] L. Chen, C. Yan, Z. Zheng, Functional polymer surfaces for controlling cell behaviors, Mater. Today 21 (2018) 38–59, https://doi.org/10.1016/J.MATTOD.2017.07.002.
[41] J. Quirós, K. Boltes, R. Rosal, Bioactive applications for electrospun fibers, Polym. Rev. 56 (2016) 631–667, https://doi.org/10.1080/15583724.2015.1136641.
[42] S.C. Wong, A. Baji, S. Leng, Effect of fiber diameter on tensile properties of electrospun poly(ε-caprolactone), Polymer 49 (2008) 4713–4722, https://doi.org/10.1016/J.POLYMER.2008.08.022.
[43] I. Keun Kwon, S. Kidoaki, T. Matsuda, Electrospun nano- to microfiber fabrics made of biodegradable copolyesters: structural characteristics, mechanical properties and cell adhesion potential, Biomaterials 26 (2005) 3929–3939, https://doi.org/10.1016/J.BIOMATERIALS.2004.10.007.
[44] P.S. Tan, S.H. Teoh, Effect of stiffness of polycaprolactone (PCL) membrane on cell proliferation, Mater. Sci. Eng. C 27 (2007) 304–308, https://doi.org/10.1016/J.MSEC.2006.03.010.
[45] P. Zuk, Y.F. Chou, F. Mussano, P. Benhaim, B.M. Wu, Adipose-derived stem cells and BMP2: Part 2. BMP2 may not influence the osteogenic fate of human adipose-derived stem cells, Connect, Tissue Res 52 (2011) 119–132, https://doi.org/10.3109/03008207.2010.484515.
[46] A.S. Badami, M.R. Kreke, M.S. Thompson, J.S. Riffle, A.S. Goldstein, Effect of fiber diameter on spreading, proliferation, and differentiation of osteoblastic cells on electrospun poly(lactic acid) substrates, Biomaterials 27 (2006) 596–606, https://doi.org/10.1016/j.biomaterials.2005.05.084.
[47] S. Gautam, A.K. Dinda, N.C. Mishra, Fabrication and characterization of PCL/gelatin composite nanofibrous scaffold for tissue engineering applications by electrospinning method, Mater. Sci. Eng. C 33 (2013) 1228–1235, https://doi.org/10.1016/j.msec.2012.12.015.
[48] N.H. Marei, I.M. El-Sherbiny, A. Lotfy, A. El-Badawy, N. El-Badri, Mesenchymal stem cells growth and proliferation enhancement using PLA vs PCL based nanofibrous scaffolds, Int. J. Biol. Macromol. 93 (2016) 9–19, https://doi.org/10.1016/j.ijbiomac.2016.08.053.
[49] L. X, L. Jy, D. Hj, D. R, M. Am, V. Ea, Influence of substratum surface chemistry/energy and topography on the human fetal osteoblastic cell line hFOB 1.19: phenotypic and genotypic responses observed in vitro, Biomaterials 28 (2007) 4535–4550, https://doi.org/10.1016/J.BIOMATERIALS.2007.06.016.
[50] L.M.C. Phillips Kl, N. Chiverton, A.L. Michael, A.A. Cole, L.M. Breakwell, G. Haddock, R.A. Bunning, A.K. Cross, The cytokine and chemokine expression profile of nucleus pulposus cells: implications for degeneration and regeneration of the intervertebral disc, Biomaterials 12 (2006) 73–84, https://doi.org/10.1089/ten.TEA.2011.0360.
[51] J. Zhang, Y. Wu, T. Thote, E. Lee, Z. Ge, Z. Yang, The influence of scaffold microstructure on chondrogenic differentiation of mesenchymal stem cells | Request PDF, Biomed. Mater. 9 (2014), 035011. https://www.researchgate.net/publication/262230266_The_influence_of_scaffold_microstructure_on_chondrogenic_differentiation_of_mesenchymal_stem_cells. (Accessed 21 April 2020). accessed.
[52] N.K. Meng Deng, Yunpeng Gu, Zhenjun Liu, Yue Qi, Gui E. Ma, Endothelial differentiation of human adipose-derived stem cells on polyglycolic acid/polylactic acid mesh - PubMed, Stem Cell. Int. 1–15 (2015). https://pubmed.ncbi.nlm.nih.gov/26106426/?from_single_result=Endothelial+differentiation+of+human+adipose-derived+stem+cells+on+polyglycolic+acid%2Fpolylactic+acid%2C+mesh&expanded_search_query=Endothelial+differentiation+of+human+adipose-derived+stem+cel. (Accessed 22 May 2020). accessed.
[53] J. Zwingmann, A.T. Mehlhorn, N. Südkamp, B. Stark, M. Dauner, H. Schmal, Chondrogenic differentiation of human articular chondrocytes differs in biodegradable PGA/PLA scaffolds, Tissue Eng. 13 (2007) 2335–2343, https://doi.org/10.1089/TEN.2006.0393.
[54] W.J. Li, Y.J. Jiang, R.S. Tuan, Chondrocyte phenotype in engineered fibrous matrix is regulated by fiber size, Tissue Eng. 12 (2006) 1775–1785, https://doi.org/10.1089/ten.2006.12.1775.
[55] D.E.I. David, J. Mooney, Robert Langer, Cytoskeletal filament assembly and the control of cell spreading and function by extracellular matrix - PubMed, J. Cell Sci. (1995) 2311–2320. https://pubmed.ncbi.nlm.nih.gov/7673351/. (Accessed 16 October 2020). accessed.
[56] L. Chen, Y. Bai, G. Liao, E. Peng, B. Wu, Y. Wang, X. Zeng, X. Xie, Electrospun poly (L-lactide)/poly(ε-caprolactone) blend nanofibrous scaffold: characterization and biocompatibility with human adipose-derived stem cells, PloS One 8 (2013), https://doi.org/10.1371/journal.pone.0071265.
[57] J.E. Babensee, L.V. McIntire, A.G. Mikos, Growth factor delivery for tissue engineering, Pharm. Res. (N. Y.) 17 (2000) 497–504, https://doi.org/10.1023/A:1007502828372.
[58] B.A. Baker, P.S. Pine, K. Chatterjee, G. Kumar, N.J. Lin, J.H. McDaniel, M.L. Salit, C.G. Simon, Ontology analysis of global gene expression differences of human bone marrow stromal cells cultured on 3D scaffolds or 2D films, Biomaterials 35 (2014) 6716–6726, https://doi.org/10.1016/j.biomaterials.2014.04.075.
[59] M. Dominici, K. Le Blanc, I. Mueller, I. Slaper-Cortenbach, F.C. Marini, D.S. Krause, R.J. Deans, A. Keating, D.J. Prockop, E.M. Horwitz, Minimal criteria for defining multipotent mesenchymal stromal cells, The International Society for Cellular Therapy position statement, Cytotherapy. 8 (2006) 315–317, https://doi.org/10.1080/14653240600855905.
[60] X. Liu, P.X. Ma, Phase separation, pore structure, and properties of nanofibrous gelatin scaffolds, Biomaterials 30 (2009) 4094–4103, https://doi.org/10.1016/j.biomaterials.2009.04.024.
[61] W. Yang, S. Both, G. van Osch, Y. Wang, J. Jansen, F. Yang, Performance of different three-dimensional scaffolds for in vivo endochondral bone generation, Eur. Cell. Mater. 27 (2014) 350–364, https://doi.org/10.22203/eCM.v027a25.